

Meenakshi Rana*, Pooja Yadav and Papiia Chowdhury

DFT investigation of nonlinear optical response of organic compound: acetylsalicylic acid

<https://doi.org/10.1515/ijmr-2021-8732>

Received December 23, 2021; accepted January 25, 2023;

published online April 24, 2023

Abstract: Nonlinear optical studies of organic compounds have been widely conducted because of its great scope in molecular engineering. In the present work, we have chosen an organic compound acetylsalicylic acid due to its non-centrosymmetric structure and presence of extended conjugated π -system. Nonlinear optical response of the probe system has been explored computationally by using density functional theory with B3LYP/6-311G++(d,p) basis set. To explore the nonlinear optical response, Mulliken charge analysis, Raman, UV-vis, nuclear magnetic resonance, molecular electrostatic potential analysis, polarizability, first order hyperpolarizability etc., have been applied for the probe molecule. Observed high value of dipole moment of optimized structure, charge transfer in the system, high Raman activity, and high value of polarizability, first order hyperpolarizability validate the strong candidature of acetylsalicylic acid to be used as a nonlinear optical active material in the future.

Keywords: Acetylsalicylic acid; Density functional theory; Hyperpolarizability; Nonlinear optical materials; Polarizability.

1 Introduction

Nonlinear optical (NLO) materials have the potential applications in the fields of photonic devices and operational information processing, such as fast data transfer, optical Frequency Conversion, electro-optical modulation, dynasty holography, laser technology, telecommunication, etc. [1–4]. Normally, geometrically asymmetry within the because of some substitution creates donor and acceptor moieties in

the material. When these types of material interact with any applied electromagnetic field, new fields in phase, frequency, and/or amplitude are generated [5]. These types of materials are called NLO active materials. A large number of organic or inorganic NLO active materials are used by the industry. Some commonly used NLO active materials are beta barium borate (BBO), urea, potassium dihydrogen phosphate (KDP), and lithium niobate (LiNbO₃) [6, 7]. Due to their high speed and high-density data processing, they have a great impact on IT and industrial applications.

NLO materials have been synthesized from a variety of materials, including molecular chromophores, polymers, semiconductors, and artificial materials like LiNbO₃ and KDP [6]. Because of qualities such as high durability, high structural flexibility, high electronic susceptibility, fast response time, easy availability, and synthesis, they have gotten a lot of attention and are favored by most scientists across the world [8, 9]. Organic NLO materials are more efficient than inorganic NLO materials due to their vast stretchability and rapid response time. In general, the presence of an electron-conjugated moiety in organic compounds with electron donor and electron acceptor groups leads to excellent NLO performance [10]. Along with this material that exhibits NLO activity is also well recognized to be non-centrosymmetric [11]. Acetylsalicylic acid has a fully non-centrosymmetric structure. The presence of extended conjugated π -system makes asymmetric charge distribution intramolecularly, which leads to improved NLO properties [12]. Keeping this in mind, we have selected acetylsalicylic acid as a probe system to detect NLO behavior.

Acetylsalicylic acid is a salicylate and is normally used as a pain reliever that also helps to lower heat and inflammation. It is normally known as Aspirin and used to treat or prevent heart attacks, strokes, and chest pain in the past (angina). The use of acetylsalicylic acid has been linked to a lower incidence of large bowel cancer [13]. Although research in animals suggests that aspirin can reduce cancer risk, there are no long-term randomized clinical trials in humans [14]. Acetylsalicylic acid is given to lower the risk of shunt blockage (CABG), after coronary artery bypass grafting [15]. In addition to its beneficial advantages, acetylsalicylic acid might have certain negative side effects [16]. Although not all of these side effects are likely to occur, if they do, medical treatment may be required.

*Corresponding author: Meenakshi Rana, Department of Physics, School of Sciences, Uttarakhand Open University, Haldwani, 263139, Uttarakhand, India, E-mail: mrana@uou.ac.in

Pooja Yadav and Papiia Chowdhury, Department of Physics and Materials Science and Engineering, Jaypee Institute of Information Technology, Noida, 201309, Uttar Pradesh, India,

E-mail: poojayadavyadav128@gmail.com (P. Yadav),

papiachowdhury@jiit.ac.in (P. Chowdhury)

In the present paper, we had done the structure optimization of acetylsalicylic acid by using density functional theory (DFT). The dipole moment, molecular electrostatic potential (MEP) analyses, and charge analysis were performed to account for the intramolecular charge transfer (ICT) within the molecule. UV-visible, Raman, IR, and NMR analysis were also reported to study the spectral activity of the compound. To check the reactivity of the system, the frontier molecular orbital (FMO) parameters were computed with the help of energies of the highest occupied molecular orbital (HOMO) and lowest unoccupied molecular orbital (LUMO). The polarizability (α) and first-order hyperpolarizability (β) parameters are observed to predict the NLO behavior of the compound.

2 Computational details

All calculations were performed with the Gaussian 09 software using density functional theory (DFT) with the B3LYP/6-311G++(d,p) standard basis set [17], and the results were interpreted by the Gauss View 5.0 [18]. The ground state geometry of the probe system is optimized without any symmetry constraints with Becke's three parameter hybrid exchange function and Lee-Yang-Parr gradient-corrected correlation functional (B3LYP) hybrid functional. B3 is Becke's 3 parameter exchange correlation functional which uses three parameters to mix in the exact Hartree-Fock exchange correlation and LYP is the Lee Yang and Parr correlation functional that recovers dynamic electron correlation. The reason for choosing B3LYP is that it is generally faster than other Hartree-Fock techniques and usually provides comparable results. The optimized structure contributes to the production of FMO energy. The other parameters are calculated by using the parameters ionization potential (IP), energy gap (ΔE), electron affinity (EA), chemical potential (μ), softness (S), and hardness (η). These parameters have been calculated using Koopman's equations:

$$IP = -E_{\text{HOMO}} \quad (1)$$

$$EA = -E_{\text{LUMO}} \quad (2)$$

$$CP = \frac{E_{\text{LUMO}} + E_{\text{HOMO}}}{2} \quad (3)$$

$$\eta = \frac{E_{\text{LUMO}} - E_{\text{HOMO}}}{2} \quad \text{and} \quad S = \frac{1}{\eta} \quad (4)$$

$$\omega = \frac{\mu^2}{2\eta} \quad (5)$$

Raman intensity is also calculated for some selected vibrational modes with the help of below-mentioned expression:

$$I = \frac{f(\nu_0 - \nu_i)^4 S_i}{\nu_i \left[1 - \exp\left(-\frac{h\nu_i}{KT}\right) \right]} \quad (6)$$

where I is the Raman intensity of the considered mode, f is a constant with a value 10^{-12} , ν_0 has value 9398.5 cm^{-1} , ν_i and S_i is the vibrational wavenumber and Raman activity of selected mode, respectively. h is the Planck's constant, c refers to the speed of light, K is the Boltzmann constant and T is the absolute temperature. To predict the system's entropy and Raman modes, frequencies are used. The first step of the frequency task is to calculate the input structure's energy. $G = H - TS$, is used to compute the entropy (S) of the probe molecule, where H is the enthalpy, G is the Gibbs free energy, and T is the temperature for the probe system.

3 Results and discussion

3.1 Structure

Optimized geometry helps in finding the net polarity of the molecule by the means of dipole moment. The high values of intramolecular interactions lead to the high value of dipole moment. The more the more dipole moment, more the compound will be polarizable. The optimized structure of acetylsalicylic acid is shown in Figure 1. Acetylsalicylic acid has a high value of dipole moment (2.196 Debye). All the bond lengths of the optimized structure of acetylsalicylic acid are mentioned in Table 1. A significant change in the bond length of the C=O and O-H bonds was observed which shows the mentioned bonds induce the reactivity of the acetylsalicylic acid. Bonds 20=21H have a bond length of 0.97 \AA and 12C-1O and 12C-4O have a bond length of 1.41 \AA and 1.22 \AA , respectively. The total energy of acetylsalicylic acid was the lowest. Therefore, it can be said that acetylsalicylic acid possesses intramolecular interactions. Better intramolecular interactions of the system are also verified by G , S , enthalpy and total energy (E) (Table 2).

3.2 Charge analysis

To understand the charge contribution corresponding to each atom of the molecule, Mulliken charge analysis plays a major role. The charge plot of acetylsalicylic acid shows the positive charge impact of H atoms and the negative charge of the O atoms. While C atoms represent both positive and negative charges. Among the H atoms, 21H shows the maximum positive charge of 0.3930 e (Table 3, Figure 2). Among the O atoms, 2O has the minimum negative charge of

Acetylsalicylic acid

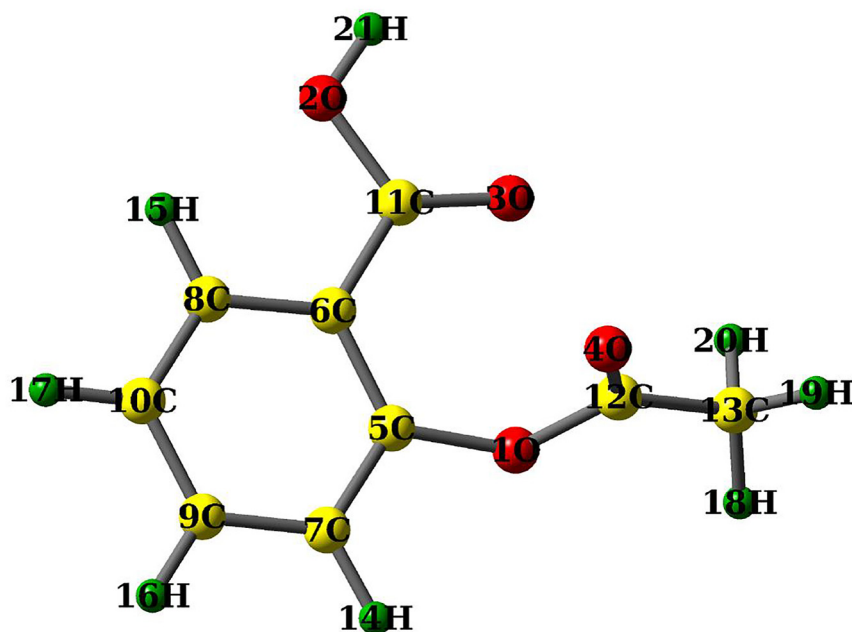


Figure 1: Optimized structure of acetylsalicylic acid by using density functional theory (DFT).

Table 1: Bond lengths of the different bonds of optimized structure of acetylsalicylic acid.

Bond	Bond length	Bond	Bond length
10–5C	1.40	11C–3O	1.23
7C–14H	1.07	6C–5C	1.40
7C–9C	1.39	11C–2O	1.38
7C–14H	1.07	21H–2O	0.97
9C–10C	1.39	1O–12C	1.41
10C–17H	1.08	12C–4O	1.22
10C–8C	1.39	12C–13C	1.49
8C–15H	1.07	13C–20H	1.09
8C–6C	1.40	13C–18H	1.08
6C–11C	1.47	13C–19H	1.08

Table 2: Zero point energy, total energy, free energy, entropy, enthalpy, Gibbs free energy, and dipole moment, of the acetylsalicylic acid.

Zero point energy (ZPE)	0.1564
Total energy (E)	–648.6650
Entropy (S)	107.869
Enthalpy (H)	–648.4959
Gibbs free energy (G)	–648.5471
Dipole moment (μ)	2.1976

Table 3: Mulliken charge values for different atom numbers of the optimized structures of acetylsalicylic acid.

S. no.	Atom number	Charge (e)
1	1O	–0.49314
2	2O	–0.55968
3	3O	–0.35524
4	4O	–0.34303
5	5C	0.29683
6	6C	–0.09696
7	7C	–0.14918
8	8C	–0.03275
9	9C	–0.09647
10	10C	–0.17345
11	11C	0.42312
12	12C	0.45299
13	13C	–0.59079
14	14H	0.16453
15	15H	0.1859
16	16H	0.16193
17	17H	0.15817
18	18H	0.21062
19	19H	0.21293
20	20H	0.23064
21	21H	0.39305

–0.559 e. The geometry has nine carbon atoms that show the charge variation. The atom 12C has a maximum positive charge of 0.45299 e and 8C shows a minimum negative charge of –0.03275 e (Table 3, Figure 2). The variation in the

charges within the molecule near the 2O–21H, 12C–4O, and 12C–1O bond lengths leads to charge delocalization from donor to acceptor moiety in the probe system leading to ICT within the molecule.

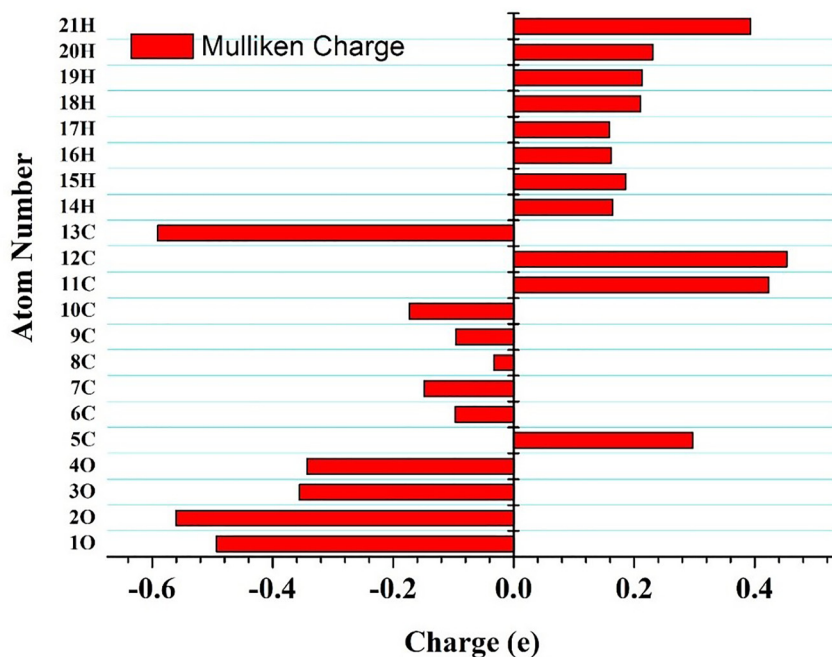


Figure 2: Mulliken charge plot for optimized acetylsalicylic acid.

3.3 Chemical reactivity

The FMO parameter helps us to get an idea about the chemical reactivity of the probe molecule [19]. In the case of Aspirin, the highest occupied molecular orbital (HOMO) and lowest unoccupied molecular orbital (LUMO) are -7.25 eV and -2.00 eV, respectively (Figure 3, Table 4). The energy gap (ΔE) value can be easily calculated by taking the difference between HOMO and LUMO energies. The lower the ΔE , the higher will be chances of ICT interactions. For the present case, the value of ΔE is 5.25 eV (Table 4). A Moderate value of ΔE reflected the chemical reactivity and optically polarizable nature of the system. Computed values of IP , χ , and EA values of the acetylsalicylic acid are 7.25 eV, 4.62 eV and 2.00 eV, respectively (Table 4). The high value of IP and χ confirms the higher reactivity of the system. The reactivity of organic molecules in a system can be classified based on parameter ω . It is a moderate electrophile if its value is less than 0.8 eV; a mild electrophile if it is between 0.8 and 1.5 eV; and a heavy electrophile if it is greater than 1.5 eV. The probe system in this example has a high ω value of 6.71 eV (Table 4), suggesting a significant electrophile presence.

The HOMO–LUMO surface over the molecule is shown in Figure 3. The donor and acceptor orbitals are located, respectively, by HOMO–LUMO surfaces in the molecular orbital wave function. The participation of the C=O and O–H bonds in the acetylsalicylic acid is demonstrated by

the HOMO–LUMO surfaces. The molecular orbital analysis reveals the existence of intramolecular interactions within the acetylsalicylic acid.

3.4 Vibrational analysis

The vibrational modes of acetylsalicylic acid are computed to study more about its spectroscopic properties [20]. The Raman spectra aid in the investigation of a compound's polarizing capacity, which leads to the compound's NLO behavior [21, 22]. Table 5 shows the computed vibrational modes for acetylsalicylic acid.

The C–H vibrations are generally observed among the modes with a frequency between 3000 and 3300 cm^{-1} . For the acetylsalicylic acid molecule, the symmetric linear stretching (ν_{CH}) modes of C–H vibrations are observed for the frequencies 3050 cm^{-1} , 3213 cm^{-1} and 3229 cm^{-1} (Figure 4). While the asymmetric linear stretching (α_{CH}) of the bond at frequency 3196 cm^{-1} . The OH symmetric linear stretching vibration (ν_{OH}) is observed at 3662 cm^{-1} . All these Raman stretching modes for the selected modes are quite high, indicating acetylsalicylic acid's high polarising ability. All of the IR and Raman modes show a high degree of conjugation in a molecule, which is accountable for acetylsalicylic acid's NLO behavior. Thus, the vibrational analysis also concludes the high hyperpolarizability and thus high NLO activity of acetylsalicylic acid.

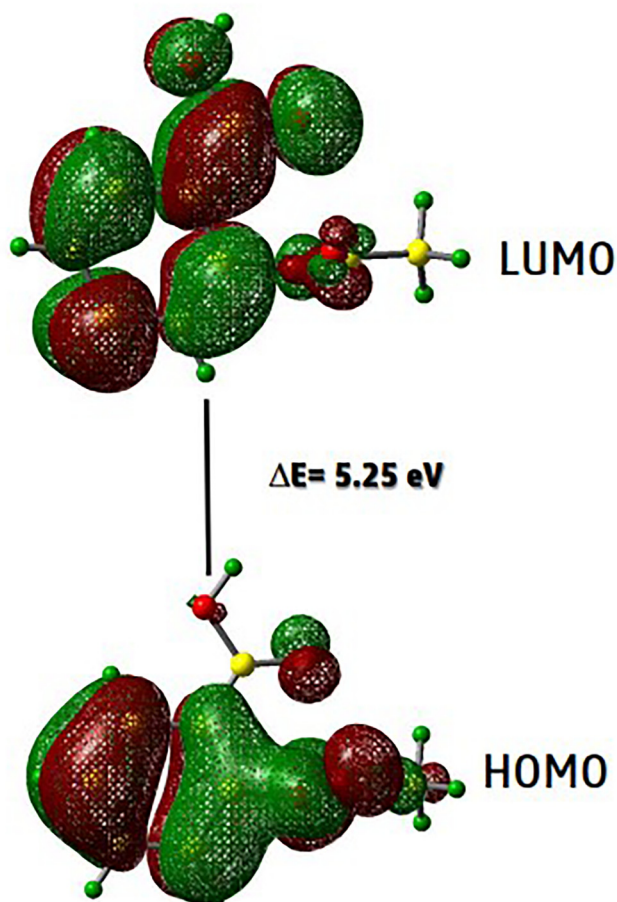


Figure 3: HOMO–LUMO diagram for acetylsalicylic acid showing an energy gap of 5.25 eV.

Table 4: Chemical parameters of acetylsalicylic acid (all values are in eV and S is in $(\text{eV})^{-1}$).

S no.	Molecular property	Values
1.	HOMO	−7.25
2.	LUMO	−2.00
3.	Energy gap (ΔE)	5.25
4.	Ionization potential (IP)	7.25
5.	Electron affinity (EA)	2.00
6.	Chemical potential (CP)	−4.62
7.	Electronegativity (χ)	4.62
8.	Hardness (η)	2.62
9.	Softness (S)	0.38
10.	Electrophilicity index (ω)	6.71

3.5 MEP analysis

MEP surface by using color code provides the electronic distribution within the Aspirin. It provides the reactive sites of the molecule [23]. The red and yellow color of the MEP

Table 5: Computational Raman modes of acetylsalicylic acid show some selected modes with frequency and their corresponding Raman activity.

S. no.	Modes	Frequency (a.u.)	Raman activity	IR intensity
1.	ν_{CO}	1690	72.10	362.34
2.	ν_{CH}	3050	135.18	1.3
3.	α_{CH}	3196	136.37	21.0
4.	ν_{CH}	3213	135.18	8.0
5.	ν_{CH}	3229	118.34	3.4
6.	ν_{OH}	3662	160.59	62.12

was due to the electrophilic atoms. While the blue color of the MEP imparts the nucleophilic region presence of the system. The occurrence of red and blue color shows the presence of both electrophilic and nucleophilic parts of the acetylsalicylic acid molecule (Figure 5).

The settlement of the red-colored surface over 12C–10 and 12C–40 bonds indicates the electron-deficient nature of C=O bonds. This might be due to the involvement of electron-withdrawing oxygen atoms. The 2O=21H bond behaves as the electron-rich moiety and impart electron donation. This shows the presence of donor and acceptor groups in the probe system. The existence of these regions confirms the high degree of electrostatic interactions within the molecule. The variation of the electronic distributions within the molecule gives a possibility of the molecule being the NLO active molecule.

3.6 UV–vis spectral analysis

To investigate the electronic properties of the system, UV–vis analysis have been performed [24]. The UV–vis spectra of acetylsalicylic acid show strong absorption bands at a wavelength ranging between 240 and 300 nm (Figure 6). Transition mechanism of acetylsalicylic acid is used to understand the electronic transitions from S_0 to different excited states S_1 , S_2 , and S_3 . We have observed the highest oscillator strength value of 0.0269 for $S_0 \rightarrow S_2$ transition at 267.42 nm wavelength. Transitions $S_0 \rightarrow S_1$ and $S_0 \rightarrow S_3$ have oscillator strengths of 0.0223 and 0.0017 and wavelengths 275.96 nm, and 245.70 respectively (Table 6). The peaks are seen in the electronic transitions of π - π^* and n - π^* , which increase the interaction of the single pair (n) electrons with the π electron. These electronic transitions also impart unsaturation to the molecule and thus show acetylsalicylic acid as NLO material.

3.7 NMR analysis

Nuclear magnetic resonance analysis (NMR) is computed by gauge-independent atomic orbital (GIAO) for

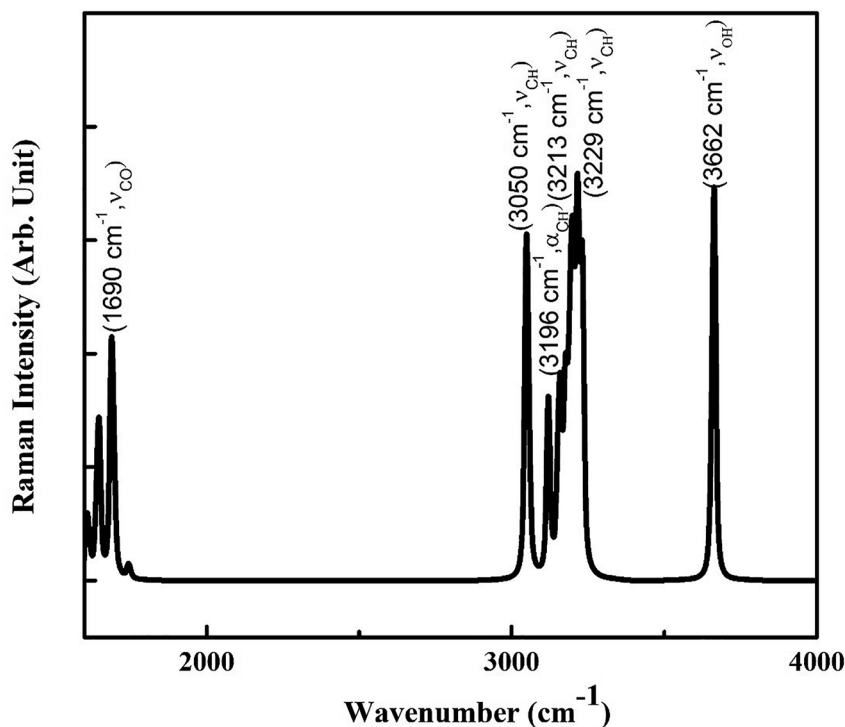


Figure 4: Computational Raman spectra of acetylsalicylic acid showing modes with maximum frequency.

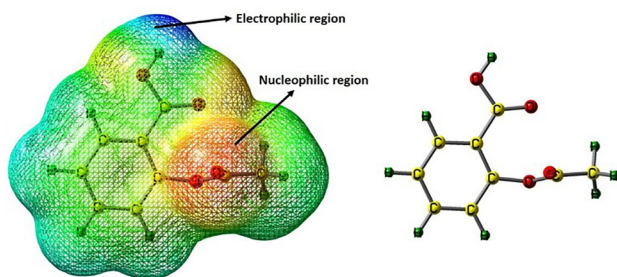


Figure 5: Molecular electrostatic potential surface of acetylsalicylic acid illustrating electrophilic region in the blue and nucleophilic region in red color.

acetylsalicylic acid [25]. The NMR study has been performed for the structural analysis of the compound [25]. Chemical shifts for ^{13}C and ^1H in ppm are reported in Table 7. Chemical shifts for aromatic carbons are observed in a normal range of 100–150 ppm [25]. The computed values of chemical shifts for aromatic carbons 5C, 6C, 7C, 8C, 9C, 10C, 11C, 12C and 13C values are obtained as 157.23 ppm, 118.44 ppm, 123.88 ppm, 132.09 ppm, 133.68 ppm, 123.91 ppm, 170.63 ppm, 178.96 ppm and 115.72 ppm (Figure 7). For 15C of the Aspirin, the shift is reported to be lowest. On the other hand, ^1H atoms show quite lower values of

chemical shift. The electrophilic group shows a shielding effect, which results in lower values of chemical shift due to the connection of hydrogen. Hydrogen atoms 14H, 15H, 16H, 17H, 18H, 19H, 20H and 21H bonded to aromatic carbons possess the chemical shift values as 6.17 ppm, 7.47 ppm, 6.56 ppm, 6.30 ppm, 1.45 ppm, 0.97 ppm, 2.18 ppm, and 5.10 ppm, respectively.

3.8 Polarizability analysis

The polarisation of a molecule influences its scattering cross-sectional strength in the presence of an applied electric field and accounts for its NLO behaviour [26, 27]. The calculation of total moment of dipole (μ_{total}), total isotropic polarisation (α_{total}), polarisation anisotropy ($\Delta\alpha$) and first order hyperpolarizability (β_{total}) other parameters is introduced to check different interactions arises from the relationship between nucleus and electron interactions. The greater the electron cloud density, the greater the atom shielding. Molecules with a large number of electrons have diffused electron clouds, making them susceptible to polarisation by external electric fields. To understand the compound diffusion of the electron cloud, polarizability parameters were calculated. The following expressions help to calculate the μ_{total} , α_{total} , $\Delta\alpha$ and β_{total} :

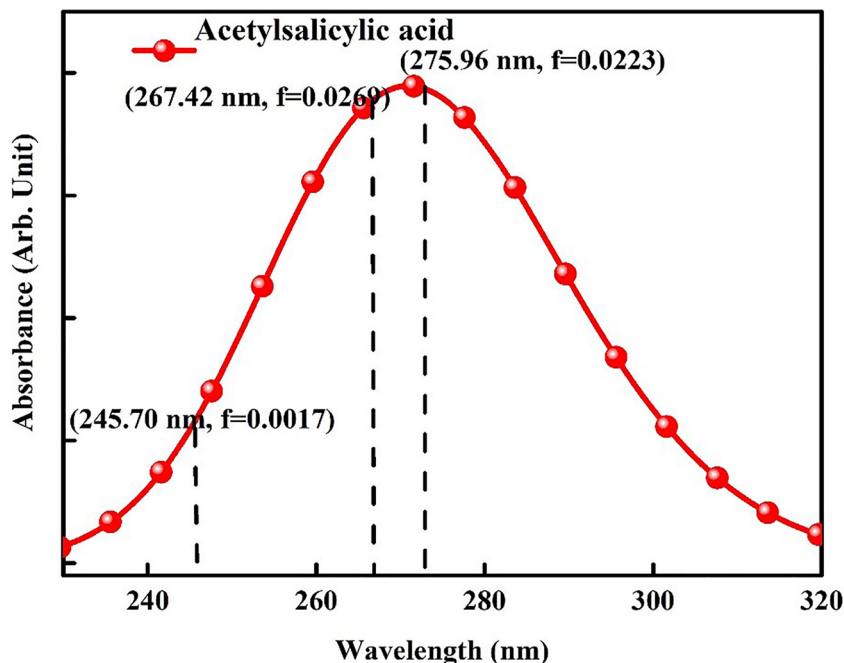


Figure 6: Computational UV-vis spectra of acetylsalicylic acid with oscillator strength.

Table 6: UV-vis absorption data of acetylsalicylic acid with transition levels and oscillator strength.

		Theoretical			
		Transition	λ (nm)	E (eV)	f
Absorption		$S_0 \rightarrow S_1$	275.96	4.4928	0.0223
		$S_0 \rightarrow S_2$	267.42	4.6363	0.0269
		$S_0 \rightarrow S_3$	245.70	5.0461	0.0017

Table 7: Computational chemical shifts of ^1H and ^{13}C atoms of Aspirin.

Atom number	Chemical shift (ppm)	Atom number	Chemical shift (ppm)
5-C	157.23	14-H	6.1777
6-C	118.44	15-H	7.4789
7-C	123.88	16-H	6.5682
8-C	132.09	17-H	6.3097
9-C	133.68	18-H	1.4525
10-C	123.91	19-H	0.971
11-C	170.63	20-H	2.1895
12-C	178.96	21-H	5.1017
13-C	15.72		

$$\mu_{\text{tot}} = \left(\mu_x^2 + \mu_y^2 + \mu_z^2 \right)^{1/2} \quad (7)$$

$$\alpha_{\text{tot}} = \frac{1}{3}(\alpha_{xx} + \alpha_{yy} + \alpha_{zz}) \quad (8)$$

$$\Delta\alpha = \frac{1}{\sqrt{2}} \left[(\alpha_{xx} - \alpha_{yy})^2 + (\alpha_{yy} - \alpha_{zz})^2 + (\alpha_{zz} - \alpha_{xx})^2 + 6\alpha_{xz}^2 + 6\alpha_{xy}^2 + 6\alpha_{yz}^2 \right]^{1/2} \quad (9)$$

where α_{xx} , α_{yy} , and, α_{zz} are the tensor components of polarizability.

For the present case, the value of μ_{total} is 2.19 Debye gives us the idea that acetylsalicylic acid has a large diffused electron cloud which indicates a strong possibility of strong intramolecular interaction [28]. The value of μ_{total} for the probe system is found to be higher than that of urea (1.52 Debye). This comparison suggested that acetylsalicylic acid has a stronger polarity and reactivity. Calculated values of α_{total} and $\Delta\alpha$ are found to be 15.56×10^{-24} esu and 37.00×10^{-24} esu (Table 8). Which is quite high from the value of α_{total} for Urea i.e., 5.664×10^{-24} esu. This rise in values of α_{total} and $\Delta\alpha$ can be expected due to donor and acceptor groups in the acetylsalicylic acid molecule. The presence of these groups leads to an increase in the values of isotropic polarizability. We have also calculated the β to validate the NLO behavior of our compound. The value of $\langle\beta\rangle$ is computed by the below-given Equation (10).

$$\langle\beta\rangle = \left[(\beta_{xxx} + \beta_{xyy} + \beta_{xzz})^2 + (\beta_{yyy} + \beta_{yzz} + \beta_{yxx})^2 + (\beta_{zzz} + \beta_{zxx} + \beta_{zyy})^2 \right]^{1/2} \quad (10)$$

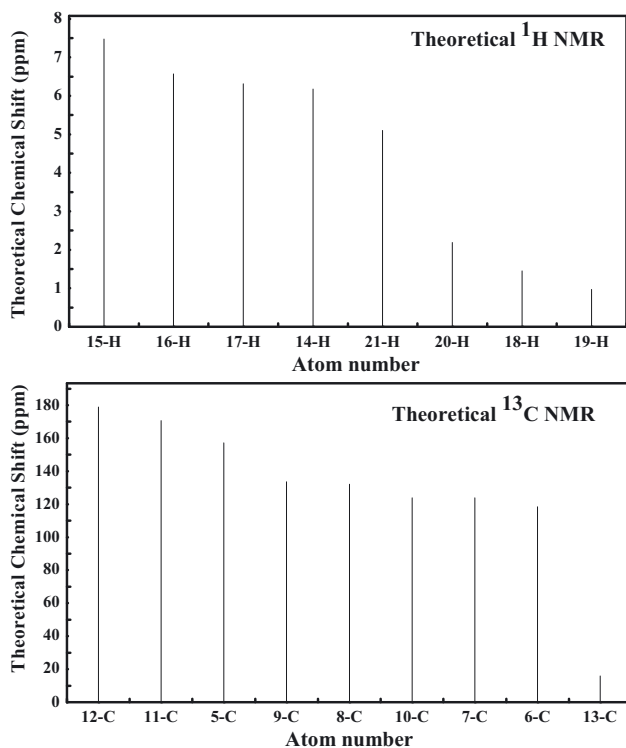


Figure 7: Computational chemical shift of H and C atoms of Aspirin.

Value for the β is computed as 1.80×10^{-30} esu (Table 8). The value of β for acetylsalicylic acid is comparable to that of urea. All these results validate the strong NLO activity of acetylsalicylic acid system.

4 Conclusions

In the present work, an investigation of NLO properties for the acetylsalicylic acid probe system is carried out using DFT calculation. The low values of bond lengths and bond angles in the probe system justify the strength of the bonds and angles within the system. The occurrence of charge distribution was established from Mulliken charge, MEP map, and molecular orbital parameters. High values of IP (7.25 eV) and χ (2.00 eV), represent the possibility of easy drifting of the electron cloud from the nucleophilic part to the electrophilic part within the probe system. Conjugated- π electrons in the probe system lead to the formation of Raman modes with high intensity. The $\pi-\pi^*$ and $n-\pi^*$ electronic transitions revealed by UV-vis spectra validate the high polarizability of the acetylsalicylic acid molecule. The band gap between the HOMO-LUMO molecules was highly related to the simulated UV-vis spectra. The NMR shifts of the ¹³C and ¹H atoms of the acetylsalicylic acid molecule suggested the delocalization of the σ and σ^* electrons. The title compound's hyperpolarizability values were significantly higher than those of the reference materials. The title compound's strong hyperpolarizability values demonstrated its high NLO activity and suitability for use in the design and development of NLO materials in near future.

Author contributions: Meenakshi Rana: Data curation, Writing-Original draft preparation, Visualization, Investigation, Software, Validation. Pooja Yadav: Conceptualization, Writing and Editing. Papia Chowdhury: Conceptualization, Methodology, Writing-Reviewing and Editing, Supervision

Table 8: Computed values of dipole moment, polarizability and first order hyperpolarizability of acetylsalicylic acid (dipole moment in Debye and all tensor components are in a.u. and μ_{total} , α_{total} , $\Delta\alpha$ and β_{total} in esu).

Component	Aspirin	Component	Aspirin	Component	Aspirin
μ_x	-0.663	α_{xx}	138.30	β_{xxx}	-124.50
μ_y	-1.06	α_{yy}	8.23	β_{yyy}	37.58
μ_z	-0.543	α_{zz}	116.94	β_{zzz}	125.76
μ_{total}	2.19	α_{xy}	-7.77	β_{xyy}	190.27
		α_{xz}	4.41	β_{xxy}	59.78
		α_{yz}	59.86	β_{xxz}	0.821
		α_{total}	15.56×10^{-24} esu	β_{xzz}	-40.21
		$\Delta\alpha$	37.00×10^{-24} esu	β_{yzz}	18.9
				β_{yyz}	-19.90
				β_{xyz}	-21.13
				β_{total}	1.805×10^{-30} esu

Research funding: None declared.

Conflict of interest statement: The authors declare that they have no known competing financial interests or personal relationships that could have appeared to influence the work reported in this paper.

References

1. Prasad P. N., Williams D. J. Introduction to nonlinear optical effects. In *Molecules and Polymers*; Wiley: New York, 1991.
2. Kuhn H. J., Robillard J. *Nonlinear Optical Materials*; CRC Press: USA, 1991.
3. Ashwell G. J., Hargreaves R. C., Baldwin C. E., Bahra G. S., Brown C. R. *Nature* 1992, 357, 393–395. <https://doi.org/10.1038/357393a0>.
4. Hunt J. H. *Nonlinear Optics*; Wiley Online Library: OSA, Washington, DC, 2021.
5. Brodie G. Energy transfer from electromagnetic fields to materials. In *Electromagnetic Fields and Waves*; IntechOpen: London, UK, 2019; pp. 1–18.
6. Roth M., Tseitlin M., Angert N. *Glass Phys. Chem.* 2005, 31, 86. <https://doi.org/10.1007/S10720-005-0028-6>.
7. Undavalli G., Joseph M., Arjun K. K., Philip R., Anand B., Rao G. N. *Opt. Mater.* 2021, 115, 111024. <https://doi.org/10.1016/j.optmat.2021.111024>.
8. Wu H., Pan S., Poeppelmeier K. R., Li H., Jia D., Chen Z., Fan X., Yang Y., Rondinelli J. M., Luo H. *J. Am. Chem. Soc.* 2011, 133, 7786–7790. <https://doi.org/10.1021/ja111083x>.
9. Shanmugam G., Brahadeeswaran S. *Spectrochim. Acta A.* 2012, 95, 177–183. <https://doi.org/10.1016/j.saa.2012.04.100>.
10. Hochberg M., Baehr-Jones T., Wang G., Shearn M., Harvard K., Luo J., Chen B., Shi Z., Lawson R., Sullivan P., Jen A. K., Dalton L., Scherer A. *Nat. Mater.* 2006, 5, 703. <https://doi.org/10.1038/nmat1719>.
11. Tamer O., Dege N., Demirtas G., Avci D., Atalay Y., Macit M., Agar A. *Spectrochim. Acta Part A* 2014, 117, 13. <https://doi.org/10.1016/j.saa.2013.07.098>.
12. Tamer O., Avci D., Atalay Y. *J. Mol. Struct.* 2015, 1098, 12.
13. Rosenberg L., Palmer J. R., Zauber A. G., Warshauer M. E., Stolley P. D., Shapiro S. *J. Natl. Cancer Inst.* 1991, 83, 355–358. <https://doi.org/10.1093/jnci/83.5.355>.
14. Elwood P. C., Gallagher A. M., Duthie G. G., Mur L. A., Morgan G. *Lancet* 2009, 373, 1301. [https://doi.org/10.1016/S0140-6736\(09\)60243-9](https://doi.org/10.1016/S0140-6736(09)60243-9).
15. Grinshtein Y. I., Savchenko A., Kosinova A. A., Goncharov M. D. *Pharmaceuticals* 2020, 13, 178. <https://doi.org/10.3390/ph13080178>.
16. Hansson L., Zanchetti A., Carruthers S. G., Dahlöf B., Elmfeldt D., Julius S., Ménard J., Rahn K. H., Wedel H., Westerling S. *Lancet* 1998, 351, 1755. [https://doi.org/10.1016/s0140-6736\(98\)04311-6](https://doi.org/10.1016/s0140-6736(98)04311-6).
17. Frisch M. J. *Gaussian 09, Revision B.01*; Gaussian Inc.: Wallingford CT, 2010.
18. Nielsen A. B., Holder A. J. *Gauss view 5.0, User's Reference*; GAUSSIAN Inc.: Pittsburgh, 2009.
19. Sebastianelli P., Pereyra R. G. *Int. J. Quant. Chem.* 2020, 120, e26060. <https://doi.org/10.1002/qua.26060>.
20. Nataraj A., Balachandran V., Karthick T. *J. Mol. Struct.* 2012, 1022, 94. <https://doi.org/10.1016/j.molstruc.2012.04.056>.
21. Catalan J., Perez P., del Valle J. C., De Paz J. L., Kasha M. *Proc. Natl. Acad. Sci.* 2002, 99, 5799. <https://doi.org/10.1073/pnas.052703999>.
22. Govindarajan M., Karabacak M. *Spectrochim. Acta Part A* 2012, 96, 421. <https://doi.org/10.1016/j.saa.2012.05.067>.
23. Kumar A., Deval V., Tandon P., Gupta A., D'silva E. D. *Spectrochim. Acta Mol. Biomol. Spectrosc.* 2014, 130, 41. <https://doi.org/10.1016/j.saa.2014.03.072>.
24. Rana M., Singla N., Chatterjee A., Shukla A., Chowdhury P. *Opt. Mater.* 2016, 62, 80. <https://doi.org/10.1063/1.5120919>.
25. Günther H. NMR spectroscopy: basic principles, concepts and applications. In *Chemistry*; John Wiley & Sons: USA, 2013.
26. Jasmine G. F., Amalanathan M., Roy S. D. *J. Mol. Struct.* 2016, 1112, 63. <https://doi.org/10.1016/j.molstruc.2016.02.013>.
27. Christiansen O., Gauss J., Stanton J. F. *Chem. Phys. Lett.* 1999, 305, 147. [https://doi.org/10.1016/S0009-2614\(99\)00358-9](https://doi.org/10.1016/S0009-2614(99)00358-9).
28. Sun Y., Chen X., Sun L., Guo X., Lu W. *Chem. Phys. Lett.* 2003, 381, 397. <https://doi.org/10.1016/j.cplett.2003.09.115>.